JOURNAL OF MATERIALS SCIENCE **40** (2005) 6099–6104

The kinetics of isothermal cold crystallization and tensile properties of poly(ethylene terephthalate)

R. M. R. WELLEN, M. S. RABELLO
Department of Materials Engineering, Federal University of Campina Grande, Av. Aprigio Veloso, 882, Campina Grande, PB, Brazil
E-mail: marcelo@dema.ufcg.edu.br

Published online: 8 September 2005

The exothermic peak that is frequently observed during the heating scan of a differential scanning calorimetry (DSC) experiment of poly(ethylene terephthalate) (PET) is due to a cold crystallization process, originating from the rearrangement of amorphous regions into a crystalline phase. In this work the isothermal cold crystallization kinetics of PET was investigated by using DSC, X-ray diffraction and tensile experiments. The isothermal crystallization rate was determined as a function of temperature, and the Avrami analysis was conducted. The results showed that at low temperatures the cold crystallization is a two-regime process, whereas at high temperatures just one stage is observed. The rate constant for isothermal crystallization K increased and the half time of crystallization $(t_{1/2})$ decreased with increasing crystallization temperature. The Avrami exponent n was close to 2, and this corresponds to a disc-like morphology formed by heterogeneous nucleation. Cold crystallization increased the crystallinity and therefore the tensile properties of the samples were enhanced.

1. Introduction

Poly(ethylene terephthalate) (PET) is a highly versatile thermoplastic with excellent thermal and chemical resistance and good mechanical performance. PET has a very high technological and commercial importance, being extensively used in the manufacture of products like synthetic fibers, films for packaging, bottles for beverages and engineering components.

With a regular molecular structure, PET can crystallize if cooled slowly from the melt. If quenched, however, it is obtained in the amorphous state because of its slow rate of crystallization. If the amorphous PET in the solid state is heated slowly above its glass transition temperature (T_g), crystalline structures are formed when the molecules have sufficient kinetic energy to start the crystal growth. This phenomenon occurs in a range of temperature between T_g and T_m, and is commonly known as cold crystallization. In DSC scans the cold crystallization is represented by an exothermic peak as shown in the example of Fig. 1.

The properties of crystalline polymers like PET depend significantly on the size and shape, orientation and perfection of the crystallites as well as on the degree of crystallinity. As a consequence, to enhance the physical and mechanical behaviour of the product the understanding of the crystallization kinetics and morphological characteristics of the material is highly desirable. A great deal of effort has been given to study the microstructure, crystallization and melting behaviour of PET under different conditions [1–19].

Although the cold crystallization of PET has been used in industry to obtain larger stiffness and resistance in injection moulded parts, very few studies have been developed to investigate the kinetics and mechanisms of cold crystallization [3–5] and no report has been seen by the present authors that deals with the relationship between cold crystallization kinetics and mechanical properties. The evaluation of the kinetics of cold crystallization has also much importance in processing techniques like injection blow moulding and thermoforming, where the premature crystallization hinders the forming stage and thus is one of the main consequences of processing faults. This paper aims to study the kinetics of cold crystallization of PET under isothermal conditions, analysing the variables that influence the processing and the consequent effects in some properties of the polymer.

2. Experimental

2.1. Materials

Poly(ethylene terephthalate) was supplied by Terphane Ltda (Brazil) in the form of amorphous sheets 0.5 mm thick produced by extrusion without further stretching. The base polymer has an intrinsic viscosity of 0.7 dL/g

0022-2461
DOI: 10.1007/s10853-005-3173-3

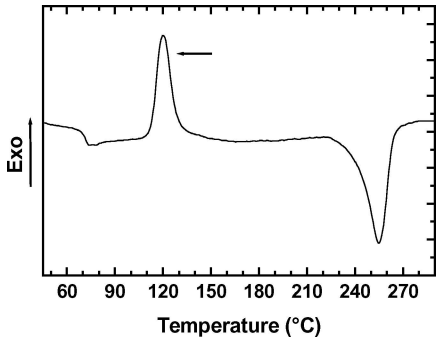

Figure 1 DSC heating scan of an amorphous PET. The arrow indicates the cold crystallization peak.

(0.07 m^3/kg) in ortho-chlorine-phenol. No additive to enhance crystallinity was added.

2.2. Crystallization kinetics

Differential scanning calorimetry (DSC) measurements were carried out using a Shimadzu DSC-50 equipment. The isothermal cold crystallization experiments were done by fast heating (∼100°C/min) the samples from room temperature to the target crystallization temperature (ranging from 100 to 150°C, at every 2.5°C). During crystallization, an exotherm was registered as a function of time, as long as no variation in the baseline was observed. From the exotherms the kinetic data were obtained as described in the following section.

2.3. Structure and properties of cold crystallized PET

To analyse the effects of cold crystallization in mechanical properties, amorphous sheets of PET (0.5 mm thick) were heated in a hydraulic press under a pressure of ∼50 MPa for various crystallization times, ranging from 1 to 120 min. The tensile properties were evaluated using a Testometric Micro 350 equipment operating at a crosshead speed of 5 mm/min and 23°C. The data were analysed according to the ASTM D 638 and the results reported represent the average of six experiments. The Young's modulus was taken as the slope of the stress-strain curve, at 0.5% strain. The structures of these cold crystallized samples were analysed by DSC and X-ray diffraction. DSC experiments were carried out under nonisothermal conditions, from room temperature to complete melting, with a heating rate of 10°C/min. X-ray diffraction analyses were done in a Siemens D5000 X-Ray Diffractometer operating at 40 kV, with 2θ ranging from 0 to 90° with a scanning rate of 0.02°/s.

3. Kinetics of crystallization

The study of crystallization kinetics of polymeric materials under isothermal conditions for various modes of nucleation and growth is usually approximated using a classical Avrami equation [20–22]. This equation was derived by assuming random nucleation, a constant growth rate, and a constant rate of nucleation (or a constant nucleation density). The general form of the Avrami expression is given in Equation 1

$$1 - X(t) = \exp(-Kt^n) \tag{1}$$

where $X(t)$ is the fractional crystallinity attained at a partial time t; n is the Avrami exponent, which depends both on the nature of nucleation and on the growth geometry; K is the overall crystallization rate constant.

In DSC isothermal crystallization analyses, the fractional crystallinity $X(t)$ is taken as the ratio of the area under the exothermic peak at a crystallization time t and the total area under the exothermic peak when the crystallization is complete:

$$X(t) = \frac{\int_0^t (dH_c/dt)dt}{\int_0^\infty (dH_c/dt)dt} \tag{2}$$

For Equation 2: $t = 0$ was established as the time when thermal equilibrium is reached, $t = \infty$ as the end of the crystallization process, and $\frac{dHc}{dt}$ as the heat flux rate.

Equation 2 can be rewritten as a ratio of areas:

$$X(t) = \frac{A_t}{A_\infty} \tag{3}$$

where A_t is the partial area under the crystallization peak at time t; A_∞ is the total area under the crystallization peak when the process is complete. $X(t)$ is the fractional crystallinity attained at each instant in relation to the total crystallinity, thus ranging from 0 and 1.

Equation 1 can be linearized and rewritten as the double logarithmic form, as follows:

$$\log[-\ln(1 - X(t))] = \log K + n \log t \tag{4}$$

If the Avrami equation is valid, then a plot of log [−ln $(1 - X(t)]$ vs. log(t) gives a straight line, and the values of K and n can be obtained directly from the slope and intercept of the best-fit line.

The Avrami plots sometimes show a two-stage process [23]. It is usual to distinguish the crystallization behaviour at the first stage, i.e., before the kinetic plot deviates markedly from the theoretical isotherm, as the primary crystallization, which consists of the outward growth of the lamellar stacks. When impingement at the growing crystals starts to occur, the overall rate of crystallization decreases, starting the second stage of crystallization, where a deviation from linearity is seen in the Avrami plot. At this stage, the crystallization takes place within spherulites and at their borders [2, 23–25].

In isothermal crystallization studies it is also common to define the half-time of crystallization ($t_{1/2}$), as the time at which the extent of crystallization is 50% complete.

4. Results and discussion

Some DSC exotherms for isothermal crystallization of amorphous PET are shown in Fig. 2. The cold crystallization peaks are well defined, occurring within

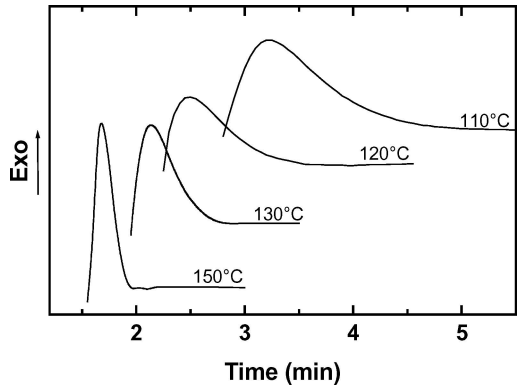

Figure 2 DSC exotherms obtained during isothermal cold crystallization of PET for selected temperatures. The experiments were actually done at temperatures ranging from 100 to 150°C, at every 2.5°C.

various time intervals according to the crystallization temperature (T_c). The displacement of the peaks to the left with increasing T_c evidences that small increments in crystallization temperature have significant influence in the phase transition process. At higher temperatures a larger molecular mobility exists, facilitating the crystalline ordering. This is opposite to the trend observed during crystallization from the melt, in which the rate of crystallization increases with decreasing temperature [2].

From DSC scans of Fig. 2, plots of partial crystallinity as a function of time were constructed for different T_c's (Fig. 3). The curves display a sigmoidal form, typical of a crystallization process without discontinuities, which occurs during phase transformation of polymers [26]. This conversion proceeds with an accelerated rate, until a pseudo-equilibrium state is reached, when the crystallization is about 90% completed. At this stage the crystallization rate decreases sharply due to crystallite impingement, rendering crystal growth increasingly difficult. This is the start of the so-called secondary crystallization, which takes place within the interlamellar region [26]. From crystallization experiments done from 110 to 150°C it is clear that the shape of the curves are rather similar, indicating that the difference in crystallization in this range of temperature is marked by differences of the nucleation and growth rates and not due to variation of the crystallization mechanism. This has also been observed previously [27].

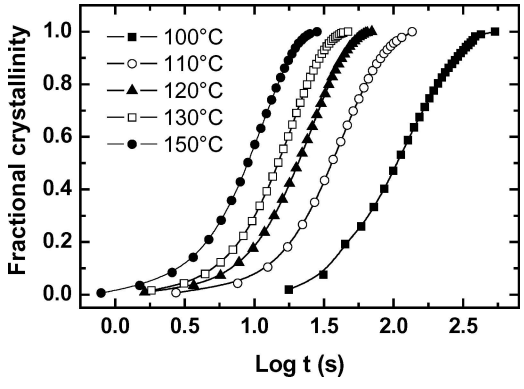

Figure 3 Development of crystallinity with time for various cold crystallization temperatures.

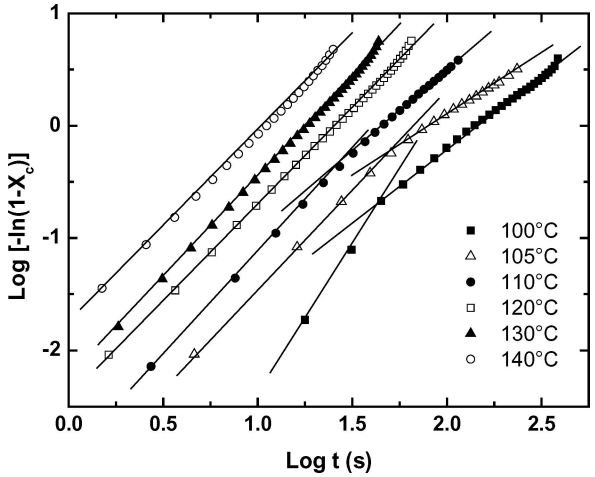

Figure 4 Some Avrami plots for isothermal cold crystallization of PET.

Some Avrami plots for isothermal cold crystallization are shown in Fig. 4. For the highest temperatures the crystallization showed only one stage (one straight line), whereas at the lowest temperatures (ca. 100–110°C) a two-stage process was observed. It is well known that the second stage of crystallization results from crystallite impingement at the end of primary crystallization, decreasing the crystallization rate as already noted (Fig. 3).

From Avrami plots the parameters n and K were estimated and are given in Table I. The exponent n had values lower than 2 for the majority of samples, which corresponds to a disk-like morphology formed by heterogeneous nucleation [26]. In a recent work on PET crystallization, Lu *et al.* [2] observed that the n-value when measured instantaneously as a function of the relative crystallinity, varies significantly (from 0.5 to 4.0) due to a progressive change in the crystallization mechanism. The value obtained by the Avrami plot represents a dominant morphology in 20–90% of the crystallization process. The values shown in Table I are similar to those obtained by other authors for cold crystallization of PET in the same range of temperature [2, 27]. The values of K increased continuously with increasing crystallization temperature mirroring the faster cold crystallization process. Fig. 5 shows the rate constant K for the full range of T_cs investigated in this work.

TABLE I Avrami parameters for selected crystallization temperatures. When Avrami plot had two stages, the parameters were taken from the first stage of cold crystallization

T_c (°C)	n	K (10^{-3} s^{-1})
100	2.6	0.010
105	1.7	0.671
110	1.8	1.24
115	1.9	1.11
120	1.7	3.80
125	1.8	4.93
130	1.8	5.60
135	1.7	7.94
140	1.9	9.06
145	1.7	15.27
150	1.7	18.94

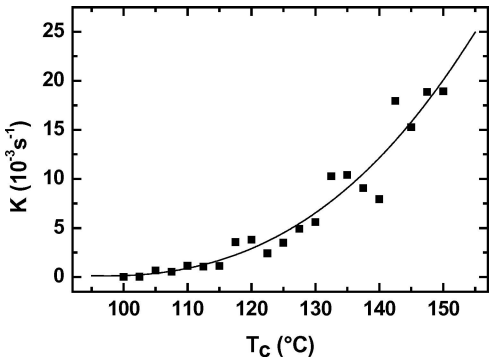

Figure 5 Effect of crystallization temperature on the rate constant K.

From the isotherms of Fig. 3, the half-time of crystallization ($t_{1/2}$) was obtained as the time to reach 50% of the final attained crystallinity and the results for different crystallization temperatures are given in Fig. 6. The rate of crystallization, defined as the reciprocal of $t_{1/2}$, is shown in Fig. 7 as a function of crystallization temperature. The crystallization rate increased markedly with increasing temperature, in agreement to the displacement of the isotherms in the direction of lower times (Fig. 3) and to the measured values of K (Table I, Fig. 5). The crystallization rate is highly dependent on T_c, due to mobility reasons. With increasing temperature the polymer segmental movement increases, facilitating molecular arrangement into a crystal lattice.

The literature, especially polymer crystallization textbooks, sometimes reports that the dependence of isothermal crystallization rate with the temperature displays a bell shape, with a maximum between T_g and T_m. The explanation is that at low temperatures the

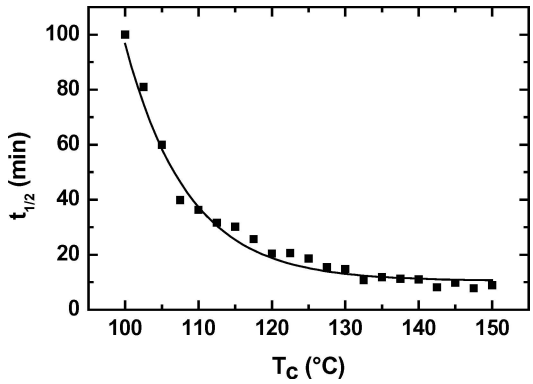

Figure 6 Half time of crystallization as a function of temperature.

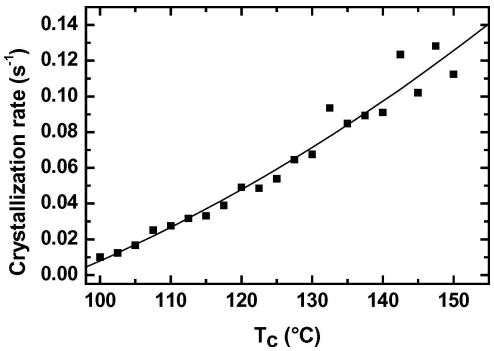

Figure 7 Effect of crystallization temperature on the cold crystallization rate of PET.

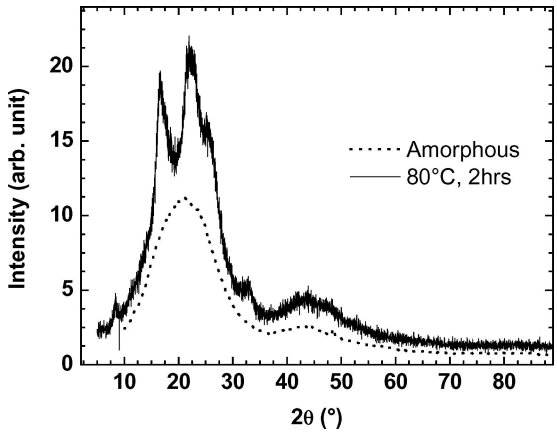

Figure 8 X-ray diffractograms for amorphous PET and after cold crystallization for 2 h at 80°C.

nucleation process governs the crystallization whereas at higher temperatures the crystalline growth becomes dominant [30]. In the results shown in Figs 5 and 7, however, this tendency is not observed, with the plot always ascending with the temperature. Actually, the maximum in the rate of crystallization is very rarely observed, and in some cases the authors join data obtained in cold crystallization (lower T_c s) and in crystallization from the melt (higher T_cs) [2].

4.1. Structure and properties of cold crystallized PET

In an attempt to develop a better understanding of the effects of cold crystallization on the structure and properties of PET, some sheets were heated in an electric press at a target crystallization temperature for various time intervals. The thermal environments in the press and in the DSC oven did not match exactly and hence a lower crystallization temperature was selected for this study. The sheets were placed between steel plates at 80°C and the effects of cold crystallization were followed. Fig. 8 displays X-ray diffractograms of PET in the amorphous state and after 2 h treatment at 80°C, when the crystallization is complete. The original polymer (i.e., amorphous) shows just a wide band, characteristic of a non crystalline material whereas diffraction peaks appear after thermal treatment, giving evidence of crystalline ordering.

After thermal treatment for different times, the samples were submitted to DSC analysis under nonisothermal conditions using a heating rate of 10°C/min, and some scans are displayed in Fig. 9. The original sample showed an exothermic peak at 115–135°C, assigned to cold crystallization occurring during the DSC analysis. A consistent reduction in the exotherm peak is noted, until it totally vanished after 2 h in the press. The smaller the exothermic peak the more intense was the cold crystallization that occurred in the press. Fig. 10 shows the variation of the cold crystallization enthalpy (ΔH_c) with the progression of the thermal treatment in the press at 80°C. This parameter displayed an accentuated decrease since the cold crystallization process partially took place during the thermal treatment. The

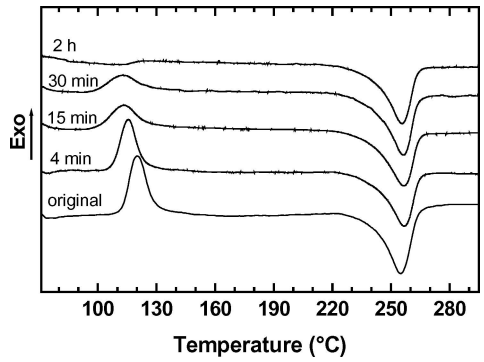

Figure 9 DSC scans of PET samples after thermal treatment at 80°C for various times.

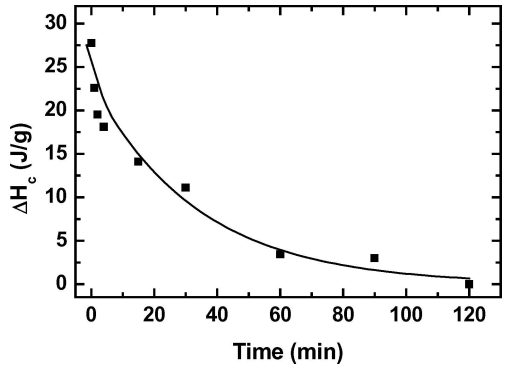

Figure 10 Crystallization enthalpy of PET samples after various times at 80°C.

shape and position of the melting peak of Fig. 9 did not show a systematic variation.

From the DSC data of Fig. 9, the degree of crystallinity after thermal treatment was obtained using the relation: $X_c = (\Delta H_m - \Delta H_c)/\Delta H_u$, where ΔH_m and ΔH_c are the melting and crystallization enthalpies respectively and ΔH_u is the melting enthalpy of the crystals (taken as 117 J/g [31]). The data obtained are shown graphically in Fig. 11. The increase in PET crystallinity is evident, although some scattering was observed for low crystallization times. A maximum in crystallinity of about 25% is achieved after ca. 90 min. This maximum depends on the inherent crystallizability of the polymer molecules, which is affected by aspects like regularity, molecular weight and polarity [30].

Considering that the crystallinity is one of the main factors that define the properties of polymers, it is

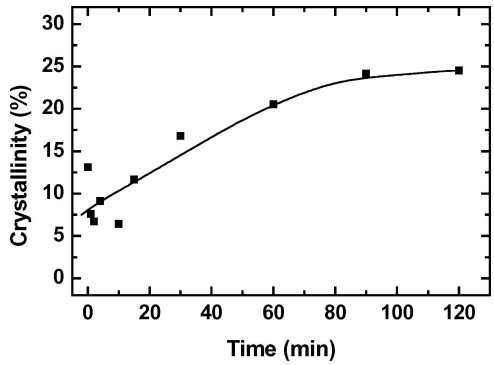

Figure 11 Crystallinity of PET samples after cold crystallization in press at 80°C.

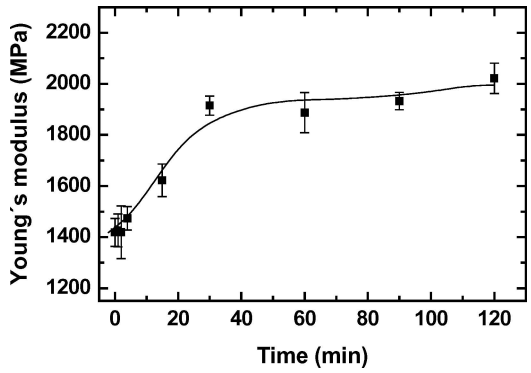

Figure 12 Effect of cold crystallization time on the Young's modulus of PET.

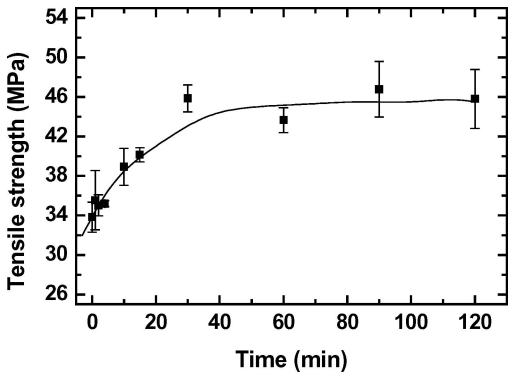

Figure 13 Effect of cold crystallization time on the tensile strength of PET.

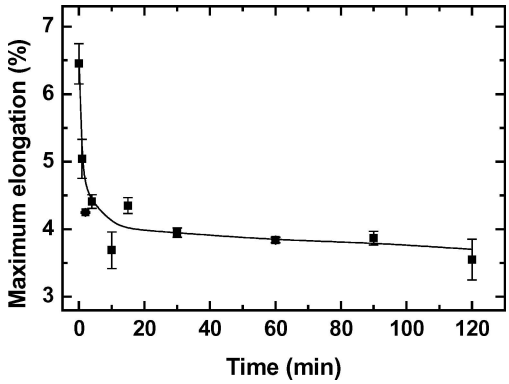

Figure 14 Maximum elongation after cold crystallization for various times.

reasonable to expect that cold crystallization may also affect the performance of PET. The tensile properties after various cold crystallization times were evaluated and the results are given in Figs 12–14. Young's modulus and tensile strength increased progressively with crystallization time, showing a curve rather similar to the one of Fig. 11. This is a strong indication of the importance of controlling bulk properties by cold crystallization. The maximum elongation (Fig. 14), on the other hand, decreased sharply with crystallization time reflecting a higher packing and lower extensibility of the crystalline phase in comparison to the amorphous region.

5. Conclusions

A study of isothermal cold crystallization of PET was carried out using DSC and the following conclusions

can be highlighted:

– The rate of cold crystallization increases sharply with increasing crystallization temperature;
– Avrami analysis indicated that at lower temperatures the crystallization occurred in two stages. In the first stage the Avrami exponent n was close to 2 for the majority of samples.
– Cold crystallization increases the degree of crystallinity of the samples reducing the crystallization enthalpy during subsequent heating. A higher degree of crystallinity changes considerably the PET tensile properties, resulting in higher elastic modulus and tensile strength and lower deformation at break.

Acknowledgments

The authors would like to thank Terphane for providing the PET sheets used in this work. RMRW is grateful to CNPq for a fellowship.

References

1. X. LU and J. N. HAY, *Polymer* **41** (2000) 7427.
2. *Idem., ibid.* **42** (2001) 9423.
3. Z. PINGPING and M. DEZHU, *Eur. Polym. J.* **33** (1997) 1817.
4. *Idem., ibid.* **35** (1999) 739.
5. *Idem., ibid.* **36** (2000) 2471.
6. W. ZHANG and D. SHEN, *Polym. J.* **30** (1998) 311.
7. L. H. PALYS and P. J. PHILLIPS, *J. Polym. Sci. Polym. Phys. Ed.* **18** (1980) 829.
8. S. TAN, A. SU, W. LI and E. ZHOU, *ibid.* **38** (2000) 53.
9. L. BOVE, C. D'ANIELLO, G. GORRASI, L. GUADAGNO and V. VITTORIA, *Polym. Adv. Tech.* **7** (1996) 858.
10. J. M. HUANG, P. P. CHU and F. C. CHANG, *Polymer* **41** (2000) 1741.
11. N. TORRES, J. J. ROBIN and B. BOUTEVIN, *Eur. Polym. J.* **36** (2000) 2075.
12. J. ZHAO, J. YANG, R. SONG, X. LINGHU and Q. FAN, *ibid.* **38** (2002) 645.
13. G. GROENINCKX, H. REYNAERS, H. BERGHMANS and G. SMETS, *J. Polym. Sci. Polym. Phys. Ed.* **18** (1980) 1311.
14. W. CHEN, E. A. LOFGREN and S. A. JABARIN, *J. Appl. Polym. Sci.* **70** (1998) 1965.
15. V. E. REINSCH and L. REBENFEIL, *ibid.* **59** (1996)1929.
16. G. GROENINCKX, H. BERGHMANS and G. SMETS, *J. Polym. Sci. Polym. Phys. Ed.* **14** (1976) 591.
17. G. GROENINCKX, H. BERGHMANS, N. OVERBERGH and G. SMETS, *ibid.* **12** (1974) 303.
18. M. XANTHOS, B. C. BALTZIS and P. P. HSU, *J. Appl. Polym. Sci* **64** (1997) 1423.
19. Z. KIFLIE, S. PICCAROLO, V. BRUCATO and F. J. BALTA-CALLEJA, *Polymer* **43** (2002) 4487.
20. M. AVRAMI, *J. Chem. Phys.* **7** (1939) 1103.
21. *Idem., ibid.* **8** (1940) 212.
22. *Idem., ibid.* **9** (1941) 177.
23. M. S. RABELLO and J. R. WHITE, *Polymer* **26** (1997) 6389.
24. S. LIU, Y. YU, Y. CUI, H. ZHANG and Z. MO, *J. Appl. Polym. Sci.* **70** (1998) 2371.
25. P. D. HONG, W. T. CHUNG and C. F. HSU, *Polymer* **43** (2002) 3335.
26. J. M. SCHULTZ, in "Polymer Materials Science" (Prentice-Hall, New Jersey, 1974).
27. V. E. REINSCH and L. REBENFEIL, *J. Appl. Polym. Sci.* **59** (1996) 1913.
28. A. M. L. M. V. SILVA, MSc Dissertation, Federal University of Rio de Janeiro, 1991.
29. M. L. DI LORENZO and C. SILVESTRE, *Prog. Polym. Sci.* **24** (1999) 917.
30. D. C. BASSET, in "Principles of Polymer Morphology" (Cambridge University Press, Cambridge, 1981).
31. G. J. M. FECHINE, R. M. SOUTO-MAIOR and M. S. RABELLO, *J. Mater. Sci.* **37** (2002) 4979.

Received 2 February
and accepted 9 May 2005